Iron Catalyzed Hydroformylation of Alkenes under Mild Conditions: Evidence of an Fe(II) Catalyzed Process

Swechchha Pandey, K. Vipin Raj, Dinesh R. Shinde, Kumar Vanka, Varchaswal Kashyap, Sreekumar Kurungot, Chathakudath Prabhakaran Vinod, and Samir H. Chikkali

J. Am. Chem. Soc., **Just Accepted Manuscript** • DOI: 10.1021/jacs.8b01286 • Publication Date (Web): 11 Mar 2018

Iron Catalyzed Hydroformylation of Alkenes under Mild Conditions: Evidence of an Fe(II) Catalyzed Process

Swechchha Pandey,[a] K. Vipin Raj,[b] Dinesh R. Shinde,[c] Kumar Vanka,[b] Varchaswal Kashyap, [b] Sreekumar Kurungot, [b] C. P. Vinod,[d] Samir H. Chikkali[a,e]*

[a]Polymer Science and Engineering Division, CSIR-National Chemical Laboratory, Dr. Homi Bhabha Road, Pune-411008, India.

[b]Physical and Materials Chemistry Division, CSIR-National Chemical Laboratory, Dr. Homi Bhabha Road, Pune-411008, India.

[c]Central NMR Facility, CSIR-National Chemical Laboratory, Dr. Homi Bhabha Road, Pune-411008, India.

[d]Catalysis Division, CSIR-National Chemical Laboratory, Dr. Homi Bhabha Road, Pune-411008, India.

[e]Academy of Scientific and Innovative Research (AcSIR), Anusandhan Bhawan, 2 Rafi Marg, New Delhi 110001, India

ABSTRACT: Earth abundant, first row transition metals offer a cheap and sustainable alternative to the rare and precious metals. However, utilization of first row metals in catalysis requires harsh reaction conditions, suffers from limited activity, and fails to tolerate functional groups. Reported here is a highly efficient iron catalyzed hydroformylation of alkenes under mild conditions. This protocol operates at 10-30 bars syngas pressure below 100 °C, utilizes readily available ligands and applies to an array of olefins. Thus, the iron precursor $[HFe(CO)_4][Ph_3PNPPh_3]$ (**1**) in the presence of triphenyl phosphine catalyzes the hydroformylation of 1-hexene (S2), 1-octene(S1), 1-decene (S3), 1-dodecene (S4), 1-octadecene (S5), trimethoxy(vinyl)silane (S6), trimethyl(vinyl)silane (S7), cardanol (S8), 2,3-dihydrofuran (S9), allyl malonic acid (S10), styrene (S11), 4-methyl styrene (S12), 4-*i*Bu-styrene (S13), 4-*t*Bu-styrene (S14), 4-methoxy styrene (S15), 4-acetoxy styrene (S16), 4-bromo styrene (S17), 4-chloro styrene (S18), 4-vinylbenzonitrile (S19), 4-vinylbenzoic acid (S20), and allyl benzene (S21) to corresponding aldehydes in good to excellent yields. Both electron donating and electron withdrawing substituents could be tolerated and excellent conversions were obtained for S11-S20. Remarkably, the addition of 1 mol% acetic acid promotes the reaction to completion within 16-24 hours. Detailed mechanistic investigations revealed *in-situ* formation of an iron-dihydride complex $[H_2Fe(CO)_2(PPh_3)_2]$ (**A**) as an active catalytic species. This finding was further supported by cyclic voltammetry investigations and intermediacy of an Fe(0)-Fe(II) species was established. Combined experimental and computational investigations support the existence of an iron-dihydride as the catalyst resting state, which then follows a Fe(II) based catalytic cycle to produce aldehyde.

INTRODUCTION

Discovered by German chemist Otto Roelen, transition metal catalyzed hydroformylation (the "oxo" process) is arguably the world's largest homogeneously catalyzed industrial process with the production of 12 million ton oxo-products per annum.[1,2] The oxo process is a powerful synthetic tool to convert alkenes into aldehydes with perfect atom economy. It has been extensively utilized to construct an array of chemical intermediates.[3] The first and second generation catalysts developed by BASF and ICI were based on cobalt.[4] However, the cobalt-catalyzed process requires harsh conditions such as 100-350 bars syngas (1:1 mixture of $CO:H_2$) pressure and around 100-200 °C temperature. Widespread academic and industrial research to address this bottleneck led to a rhodium catalyzed low-pressure oxo-process (LPO) (10-60 bars and 80-135 °C),[5] which was developed by Union Carbide and Celanese in the mid-1970s.[6] To date, terminal alkenes, internal alkenes, cyclic olefins and aromatic alkenes have been extensively hydroformylated to pharmaceuticals, fragrances and agrochemicals using the precious rhodium metal.[7] Thus, due to technical superiority, the rhodium-based LPO is still the state of the art process practiced by industry and roughly 70% of the oxo-products are produced using this process. However, the industry is increasingly being faced with the rocketing prices of rhodium due to the high demand of this metal in the automotive industry, which consumes about 80% of this metal. In addition, the natural abundance of this trace element is posing an even bigger challenge and the search for alternative metals has already begun.[8]

Iron (Fe) is an earth abundant element in contrast to precious rhodium, and its usage is justified for reasons of economic and sustainability. Iron catalyzed hydroformylation of olefins has been reported on few occasions in the past.[8] Figure 1 depicts the state of the art in iron catalyzed hydroformylation. The first example of iron catalyzed hydroformylation was reported by Reppe and Vetter. At 14% loading of $[Fe(CO)_5]$, ethylene was converted to propanol under 100-200 bars of CO pressure.[9] Note that no syngas was employed but the water gas shift reaction was anticipated to deliver the hydrogen. Similar attempts using 100 bar CO pressure (at 140 °C) were reported by Palagyi *et al.* after 30 years, but the conversion remained very low (30%).[10] Ru-Fe cluster catalyzed hydroformylation in the presence of syngas was

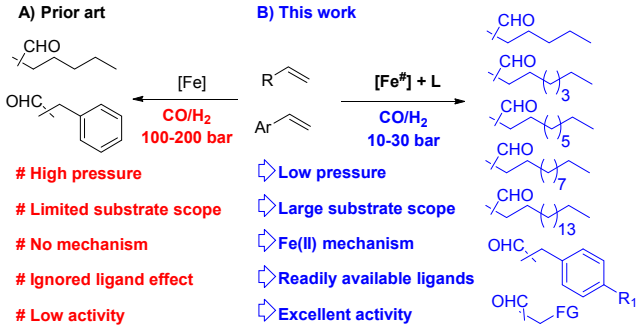

Figure 1. State of the art iron catalyzed hydroformylation (left) and present work (right) {[Fe#] = ($HFe(CO)_4^-$) (L = PPh_3/$P(OPh)_3$)}.

reported in 1992 for the first time and the TOF of 0.4-4.0 was recorded.[11] Although it was not clear which metal was responsible for the observed hydroformylation activity, a synergistic effect between the two metals was claimed to be responsible. The latest report in iron catalyzed hydroformylation was published in 2000, utilizing an isolated iron complex [Fe(η^6-CHT)(η^4-COD)], (CHT: 1,3,5-cycloheptatriene; COD: 1,5-cyclooctadiene).[12] Iron catalyzed hydroformylation of 1-hexene and styrene at 100 °C and 100 bars syngas pressure was investigated (Fig. 1, left). Thus, the iron catalyzed hydroformylation is still in its infancy and suffers from serious limitations, such as high syngas pressure, limited substrate scope, lack of understanding of ligand effects and low activities. In addition, no comprehensive picture of the mechanism of Fe-catalyzed hydroformylation exists, beyond the parallels drawn with Ru-catalyzed hydroformylation.

Herein, we describe iron catalyzed hydroformylation (HF) of olefins under mild conditions: 10-30 bars syngas pressure and below 100 °C, which falls under the purview of LPO. The generality of the approach has been demonstrated by subjecting various olefins, such as 1-octene, 1-hexene, 1-decene, 1-dodecene, 1-octadecene, trimethoxy(vinyl)silane, trimethyl(vinyl)silane, cardanol, 2,3-dihydrofuran, allyl malonic acid, styrene, 4-methyl styrene, 4-*i*Bu-styrene, 4-*t*Bu-styrene, 4-methoxy styrene, 4-acetoxy styrene, 4-bromo styrene, 4-chloro styrene, 4-vinylbenzonitrile, 4-vinylbenzoic acid, and allyl benzene to iron catalyzed hydroformylation. A Fe(II) based mechanism is proposed as predicated by DFT calculations and experimental evidence. This methodology relies on commonly available reagents, does not require harsh conditions, and uses an earth abundant, non-toxic and cheap metal, which makes this approach highly suitable for practical hydroformylation of industrially important alkenes.

RESULTS AND DISCUSSION

Hydroformylation of 1-octene. It is known that the hydroformylation reaction proceeds *via* a metal-hydride intermediate.[13] In our attempts to meet this criteria, we synthesized an iron-hydride complex $[HFe(CO)_4][PPN]$ (**1**) (where PPN = Bis(triphenylphosphine)iminium) by following a known procedure.[14] The identity of (**1**) was fully established by using a combination of spectroscopic and analytical methods. An overview of iron catalyzed reactions reported in the literature indicated that iron complexes can be activated in the presence of suitable ligands.[15] Guided by these reports, we anticipated that the best way to manipulate the reactivity of **1** would be to offer a competitive ligand to replace carbonyls and activate **1** *in situ*. Phosphorus ligands such as phosphines,[16] phosphites,[17] phosphinites,[18] diphosphines,[19] diphosphites,[1f] phosphine-phosphonite,[20] phosphine-phosphoramidite[21] and phosphine-phosphite[22] have been extensively utilized in rhodium catalyzed hydroformylation. Thus, given the success of the phosphorus ligand in hydroformylation, we zeroed in on readily accessible σ-donor ligands such as phosphines and σ-donor π-acceptor ligands such as phosphites.[23] The performance of precursor **1** in the presence of triphenyl phosphine (**L1**) and triphenyl phosphite (**L2**)

Table 1. Iron (**1**) catalyzed hydroformylation of 1-octene under mild conditons.[a]

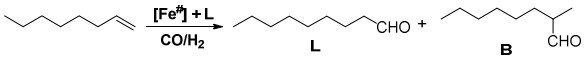

Run	L (equiv.)	Solvent	CO/H_2 (bars)	Time (h)	Conv. (%)[b]	L:B [b]
1	L1 (1)	MeOH	20	24	47	73:27
2	L1 (2.5)	MeOH	20	24	95	66:34
3	L1 (3)	MeOH	20	24	95	64:36
4	L1 (4)	MeOH	20	24	92	64:36
5	L1 (2.5)	THF	20	24	3	NA
6	L1 (2.5)	DXN	20	24	66	73:27
7	L1 (2.5)	DCM	20	24	24	63:37
8	L1 (2.5)	EtOH	20	24	17	67:33
9	L1 (2.5)	iPrOH	20	24	20	70:30
10	L1(2.5)	MeOH	30	48	90	60:40
11	L1(2.5)	MeOH	30	24	76	70:30
12	L1(2.5)	MeOH	15	24	62	67:33
13[c]	L1(2.5)	MeOH	20	24	85	67:33
14[d]	L1(2.5)	MeOH	20	24	3	74:26
15	NA	MeOH	35	24	0	NA
16	L2(1)	MeOH	20	48	18	68:32
17	L2(2.5)	MeOH	20	48	47	70:30
18	L2(3)	MeOH	20	48	27	65:35
19	L2(2.5)	MeOH	30	48	92	63:37
20	L2(2.5)	MeOH	30	24	5	76:24
21	L2(2.5)	MeOH	20	24	2	NA
22[e]	L2(2.5)	MeOH	20	24	23	68:32

[a]Conditions: **1**: 0.0077 mmol, L/M: 2.5, Sub/Fe: 100, Solvent: 1 ml, NA: Not applicable; MeOH-Methanol, THF-Tetrahydrofuran, DXN-1,4-dioxane, DCM-Dichloromethane, EtOH-Ethanol, iPrOH-Isopropanol, hardly any (~1%) hydrogenation product was detected. [b]Determined by GC. [c]Performed at 120 °C. [d]Performed at 80 °C. [e]L2 was incubated for 24 hours before addition of 1-octene.

in the iron catalyzed hydroformylation of 1-octene was evaluated and the representative catalytic data is summarized in Table 1. The catalysts were prepared *in situ* by mixing a suitable amount of the iron precursor **1** and phosphorus ligands **L1**

Table 2. Iron (**1**) catalyzed hydroformylation of alkenes in the presence of **L1**. S1: 1-octene, S2: 1-hexene, S3: 1-decene, S4: 1-dodecene, S5: 1-octadecene, S6: trimethoxy(vinyl)silane, S7: trimethyl(vinyl)silane, S8: cardanol, S9: 2,3-dihydrofuran, S10: allyl malonic acid, S11: styrene, S12: 4-methyl styrene,

S13: 4-*i*Bu-styrene, S14: 4-*t*Bu-styrene, S15: 4-methoxy styrene, S16: 4-acetoxy styrene, S17: 4-bromo styrene, S18: 4-chloro styrene, S19: 4-vinylbenzonitrile, S20: 4-vinylbenzoic acid, S21: allyl benzene.[a]

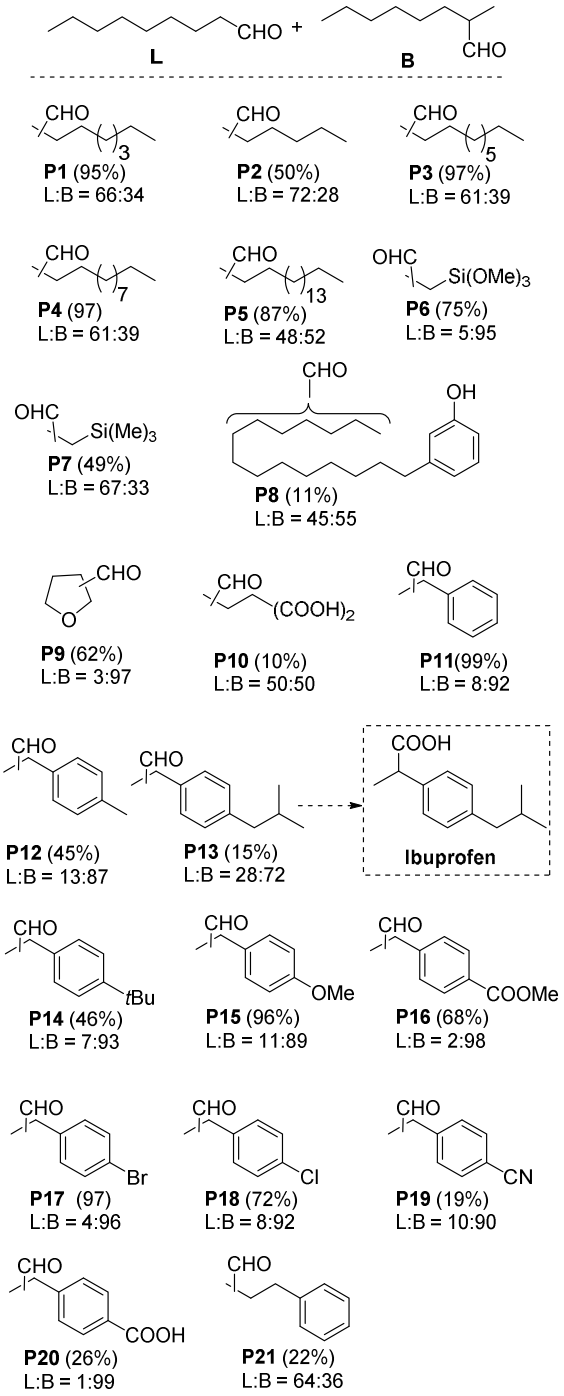

[a]Conditions: **1**: 0.0077 mmol, L/M: 2.5, Sub/Fe: 100, Solvent: 1 ml methanol, L:B = Linear:Branched, Yield (in bracket, %) determined by GC/^{1}H NMR spectroscopy, hardly any (~1%) hydrogenation product was detected.

or **L2** in the presence of syngas. Preliminary screening indicated an optimal ligand to metal ratio of 2.5 (Table 1, run 1-4).[24] Remarkably, addition of triphenyl phosphine to iron precursor **1** catalyzed the hydroformylation of 1-octene to nonanal with excellent conversion (90-95%) (Table 1, run 2-4), without any hydrogenation side reaction. In our attempts to identify the most suitable solvent, various solvents were screened (Table 1, run 5-9). Methanol was found to be the solvent of choice and none of the other solvents were as effective as methanol. Performing the hydroformylation at lower and higher syngas pressure indicated an optimal pressure of 20 bars (run 2 vs 10-12) with 95% conversion within 24 hours, without jeopardizing the regioselectivity. Increasing the temperature to 120 °C led to slightly lower conversion, but decreasing the temperature to 80 °C dramatically reduced the conversion to only 3% (Table 1 runs 13-14). In a control experiment, hydroformylation of 1-octene using precursor (**1**), in the absence of ligand, failed to produce the corresponding nonanal (Table 1, run 15). This observation clearly indicated that precursor **1** on its own is not capable of interacting with alkenes and may not be the actual active species. Thus, the control experiment accentuates the pivotal role of ligand in iron catalyzed hydroformylation, without which the iron hydride complex **1** is not active enough. Encouraged by these results, we evaluated the performance of a readily available, σ-donor π-acceptor ligand, triphenyl phosphite (**L2**).[25] Initial screening in the presence of ligand **L2** indicated an optimal ligand to metal ratio of 2.5 (Table 1, run 16-18). However, it should be noted that a longer reaction time was required to achieve reasonable conversion under identical conditions (Table 1, run 17).[24] Notably, increasing the syngas pressure to 30 bars revealed an improved yield of 92% in 48 hours (Table 1, run 19). However, performing the reaction at the same syngas pressure as in run 19 but for a shorter period of time (Table 1, run 20), lead to only 5% conversion. This anomalous behaviour could be due to the weak σ-donation and lower coordinating ability of **L2**. At a higher ligand to metal ratio, the phosphite ligands are known to be slower, leading to longer reaction times, and the behaviour noted here is in line with the previous reports.[26] Incubating **L2** for 24 hours and *in situ* addition of substrate revealed slight improvement in the activity (Table 1, run 22).

Scope of iron catalyzed hydroformylation. With optimized reaction conditions in hand, the scope of the iron catalyzed hydroformylation was examined (Table 2) and about 20 substrates were evaluated. Both aliphatic and aromatic substrates were hydroformylated with good to excellent conversion to aldehydes. The aromatic substrates exhibited slightly lower reactivity. A short chain alkene, 1-hexene, was hydroformylated under further milder conditions with 50% exclusive conversion to heptanal (Table 2, P2) along with 72% linear selectivity. Hydroformylation of long-chain alkenes is even more challenging, as their reactivity decreases with increasing carbon number and the possibility of internal isomers and corresponding aldehyde products increases.[27] With increasing chain length of the olefin, the reactivity was found to decrease.[28] Thus, at 15 bars syngas pressure and 100 °C, a C10 olefin S3 led to only 47% yield, whereas increasing the CO/H_2 pressure to 30 bars led to an improved yield of 97% (Table S3, run 2 vs 3).[29] Along the same lines, 1-dodecene (S4) and 1-octadecene (S5) displayed 97% and 87% yield respectively under identical conditions (Table S3, run 4-5).[30,31]

With this initial success, the resilience of the catalyst was examined by subjecting functional olefins to iron catalyzed hydroformylation. The catalyst was found to tolerate trimethoxy group without any hindrance and 75% conversion to aldehyde was observed (Table 2, P6). A slight change in the silane to trimethyl(vinyl)silane led to 49% conversion to alde-

hyde. A notoriously difficult cardanol (S9), which is a non-edible plant oil derived substrate, was tested in the iron catalyzed hydroformylation. Although only 11% aldehyde product could be observed, the fact that such a mixture (cardanol is mixture of three different internal olefins) could be hydroformylated indicates the potential that the iron catalyst holds. A highly challenging heterocyclic olefin, 2,3-dihydrofuran (S9), was hydroformylated to yield (62%) a highly regioseletive 3-carbaldehyde with 97% selectivity (Table 2, P9). Hydroformylation of 1,1-disubstituted difunctional olefin S10 (allyl malonic acid) lead to reduced activity and only 10% aldehyde could be observed, clearly indicating the limited functional group tolerance of the current catalytic system. On an average, aliphatic olefins were hydroformylated in 24 hours, whereas aromatic substrates required 48 or more hours. Styrene was chosen as a representative benchmark substrate and iron catalyzed hydroformylation was examined.[32] Under optimized conditions, a quantitative conversion was observed at 20 bars syngas pressure at 100 °C, with the preferred branched aldehyde formed with 92% selectivity (Table 2, P11). The reversal of regioselectivity is very commonly observed in styrenic substrates and monodentate phosphine ligands are known to preferably deliver the branched product.[33,34] Both electron donating and electron withdrawing substituents were tolerated (Table 2, P12-20). The electron donating substrates 4-methyl styrene (S12),[35,36] 4-*tert*butyl styrene (S14) demanded 30 bars syngas pressure for 45-50% conversion. To demonstrate the practical significance of this methodology, hydroformylation of S13 was performed to yield aldehyde P13 which can be eventually oxidized to yield ibuprofen (Table 2), an anti-inflammatory drug. Whereas the electron withdrawing substituents fared better and 4-bromo styrene (S17) led to full conversion at 20 bars syngas pressure (Table S3, runs 21 *vs* 15). S17 also revealed a high regioselectivity of 96% branched aldehyde (P17) with an excellent yield of 97%. Acetoxy, nitrile and carboxyl groups could be tolerated but at the cost of slightly reduced conversion to aldehyde (Table S3, run 20, 23-24).

Table 3. Acetic acid promoted iron (**1**) catalyzed hydroformylation of 1-hexene, styrene and styrene derivatives.[a]

Run	Substrate	AcOH	Time (h)	Conv. (%)[b]	L:B[b]
1[c]	S2	1	16	49	72:28
2[c]	S2	2	16	25	73:27
3[c]	S2	5	16	1	NA
4	S11	1	24	94	14:76
5	S12	1	24	32	16:84
6	S15	1	24	64	16:84
7	S17	1	24	80	8:92

[a]Conditions: **1**: 0.077 mmol, L/M: 2.5, Sub/Fe: 100, Solvent: 1 ml methanol, CO/H_2: 20 bars, Temp.: 100 °C, S2: 1-hexene, S11: styrene, S12: 4-methyl styrene, S15: 4-methoxy styrene, S17: 4-bromo styrene, NA: Not applicable; [b]Determined by GC. [c]Temp.: 80 °C.

Thus, the above observations indicate that electron poor styrene derivatives are relatively easy to hydroformylate, whereas electron rich styrenics are slightly difficult to access. While a significant amount of literature deals with the hydroformylation of vinyl aromatics, very little is known about the hydroformylation of allyl aromatics.[37] The resultant aldehydes are high value pharamaceutical intermediates.[38] As a representative case, iron catalyzed hydroformylation of allyl benzene (S21) was investigated. Precursor **1** in the presence of **L1** catalyzed the hydroformylation of allylbenzene to yield the linear selective (64%) product (P21) with a moderate conversion of 22% (Table S3, run 25).

Acetic acid promoted iron catalyzed hydroformylation. Having established iron catalyzed hydroformylation of various olefins, we pondered about the role of the solvent. It is to be noted that hydroformylation was found to take place in alcoholic solvents, suggesting active participation of the solvent. In this context, we postulated that the alcoholic solvents might be delivering a proton to precursor **1**, to generate the active species. To test our hypothesis, we investigated the effect of acidic additives on the hydroformylation activity. To our delight, the addition of 1 mol% (AcOH:[Fe] = 1:1) acetic acid was found to dramatically promote the hydroformylation reaction.[39] Initial additive screening suggested that 1 equivalent (as compared to iron precursor **1**) of acetic acid is sufficient to promote the reaction (Table 3, run 1-3). Under optimized conditions, hydroformylation of S2 led to 49% conversion within 16 hours, which otherwise required 48 hours for similar conversion without the additive (Table 3, run 1 versus Table S3 run 1). Remarkably, six fold increased activity was observed in the hydroformylation of styrene, which was completed (94% conversion) within 24 hours (Table 3, run 4), instead of the earlier 16% conversion (Table S3, run 11). Along the same lines, accelerated hydroformylation of S12, S15 and S17 was observed in the presence of acetic acid. Table 3 lists the important experiments. Thus, addition of 1 mol% (1 equivalent compared to iron precursor **1**) acetic acid promotes the hydroformylation of 1-hexene, styrene and styrene derivatives and accelerated conversion could be obtained within 16-24 hours.

Mechanistic investigations.

NMR spectroscopy. Unfolding the elementary steps in the iron catalyzed hydroformylation will be of great significance for understanding the reactivity of the iron catalyst and might unlock the synthetic potential of this earth abundant metal in hydroformylation. Primitive reports on iron catalyzed HF either refer to the ruthenium based mechanism[40] or cite the Reppe process, which proposes the CO deficient $[H_2Fe(CO)_3]$ as an active intermediate.[41] However, direct experimental or theoretical evidence for iron catalyzed HF is largely missing.

In our attempts to trap key intermediates, precursor **1** was treated with triphenyl phosphine at 45 °C and the progress of the reaction was monitored by phosphorus NMR spectroscopy. The ^{31}P resonances at 82.3 and 71.5 ppm indicated coordination of **L1** to the metal and the presence of intermediate (**i**) (Scheme1) (SI Fig. S27). The above phosphorus chemical shifts fall within the range of mononuclear iron-phosphine complexes reported earlier. Beller and co-workers in their investigation on iron catalyzed hydrogen production using formic acid reported that the coordinated phosphorus in $[Fe(CO)_3(PPh_3)_2]$ complex appear at 82.5 and 70.6 ppm.[42] Therefore, the resonance at 82.3 and 71.5 ppm observed in our investigation can be assigned to coordinated **L1**. It should be noted that the phosphine coordination was observed at an elevated temperature of 45 °C. In an ideal situation, addition of acetic acid at 45 °C would lead to the generation of intermediate **A**. However, addition of acetic acid to the above NMR

tube and recording proton NMR did not show any hydride resonance. This is most likely due to release of H_2

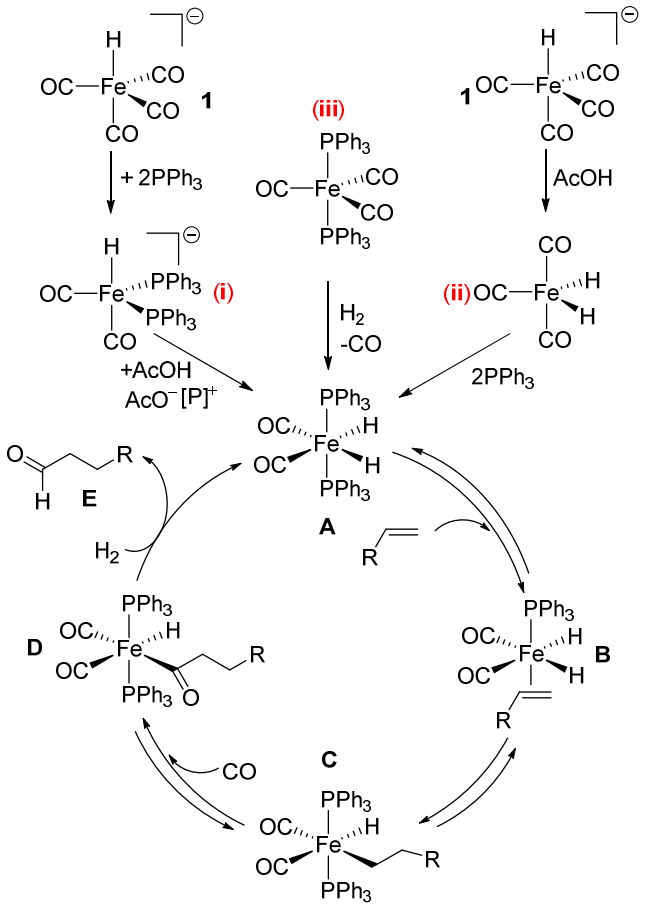

Scheme 1. Proposed catalytic cycle for iron catalyzed hydroformylation. The orientation of ligands around the metal is only for the sake of understanding and does not mean that this is the final spatial arrangement of the ligands.

from intermediate (**A**) at elevated temperature. To arrest the hydrogen release, the NMR tube with added **L1** was first heated for 16 hours at 45 °C, and then the tube was cooled to 0 °C. At this temperature, acetic acid was added to the NMR tube and a proton and ^{31}P NMR was recorded. Thus, the addition of acetic acid led to the appearance of a very weak hydride signal at -12.28 ppm (SI Fig. S30), but the intensity of the signal was so weak (even after large number of scans) that it demanded further support. In the hope of capturing intermediate **A**, compound **1** was treated with triphenyl phosphine and acetic acid was added at room temperature without heating the reaction mixture. Immediately a proton NMR was recorded, which revealed a doublet centered at -9.50 ppm (SI Fig. S33). This chemical shift can be assigned to complex **A**, which is consistent with literature reports.[43] Similar results were obtained when deuterated acetic acid (CD_3COOD) was used (SI Fig. S33R). This is most likely due to fast H-D exchange between added deuterated acetic acid and the protic solvent (methanol). In a second route to trap intermediate species **A** (scheme 1), **1** was treated with acetic acid to reveal a hydride resonance at -15.3 ppm (SI Fig. S34). Observation of the hydride resonance confirmed the formation of species (**ii**). However, addition of **L1** did not show any coordination at room temperature and heating the sample to obtain the desired coordination led to elimination of H_2. Therefore, species **A** could not be generated by following this route.[44] In a third protocol, formation of **A** was accessed by synthesizing the known iron-phosphine complex (**iii**). Isolated complex (**iii**) was treated with hydrogen gas in a high pressure NMR tube and the tube was heated to 60 °C for 16 hours. The progress of the reaction was monitored by proton and phosphorus NMR spectroscopy. ^{31}P NMR of the resultant mixture revealed a resonance at 83.1 ppm (SI Fig. S36) and the corresponding proton NMR displayed two broad singlets at -8.91 and -9.02 ppm (SI, Fig. S35). These resonances can be tentatively assigned to an iron complex that would be similar to species **A**; perhaps with a different spatial arrangement of the two hydrides. Thus, the above spectroscopic investigations suggest formation of species **A**, which might be the potential active species for hydroformylation. The intermediate thus prepared is highly unstable and only *in situ* characterization has been attempted.

Cyclic voltammetry. The interconversion of Fe(0) to Fe(II) species was further supported by cyclic voltammetry (CV) investigations. The cyclic voltamogram (CVs) of the iron precursor (**1**) was recorded before and after the addition of acetic acid in the electrolyte medium (Fig. 2).[45] Initial reduction potential for the compound (**1**) was found to be 0.43 V (*vs* Pt), which was shifted to 0.33 V (*vs* Pt) after acetic acid addition. Similarly, a shift in the oxidation peak of the precursor **1** was noted from 0.55 to 0.40 V(*vs* Pt). The above shift in the peak

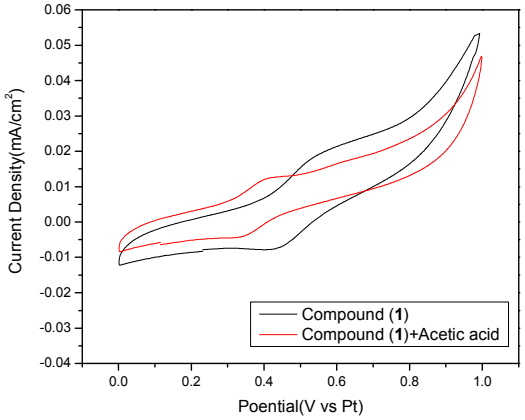

Figure 2. Cyclic voltamograms of iron precursor (**1**) (black line) and (**1**) + acetic acid (red line), recorded at 50mV/s with an electrode rotation rate of 900 rpm in 0.1 M $LiClO_4$ (solution in methanol

potential clearly indicates that the initial Fe(0) species in precursor **1** is being converted to the iron-dihydride species after the addition of acetic acid. To verify these results further, control experiments were conducted under analogous conditions. Ferrocene, ferrocene carboxylic acid, $[Fe(CO)_3(PPh_3)_2]$ and $[Fe(CO)_5]$ were selected as control samples. As can be seen in Figure S41, the ferrocene and ferrocene carboxylic acid, wherein iron is in the +2 oxidation state, displayed separate peak positions for oxidation and reduction. The shift in the peak position is related to the carboxylic group attached to the cyclopentadienyl ring.

Further, we recorded the CVs of the iron(0) compounds such as $[Fe(CO)_3(PPh_3)_2]$ and $[Fe(CO)_5]$. The CV of $[Fe(CO)_3(PPh_3)_2]$ revealed an oxidation and reduction peak at higher potential against the iron(+2) ferrocene and ferrocene carboxylic acid, whereas no peak for $[Fe(CO)_5]$ could be iden-

tified in the analogous potential range (SI Fig. S42). The anomalous behavior of the $[Fe(CO)_5]$ could be because of the homogenous ligand surrounding the metal. As evident from the control experiments outlined above, it is most likely that the Fe(0) precursor **1** is converted to Fe(II) after the addition of acetic acid. The reduction peak of the acetic acid treated compound **1** was in close resemblance with Ferrocene (0.26 V vs Pt), i.e. iron(2+). Whereas precursor **1** (0.43 V vs Pt) without acetic acid treatment resembles $[Fe(CO)_3(PPh_3)_2]$ (0.46 V vs Pt) , i.e. Fe(0).

Computational and additional experimental evidence. The existence of **A** was investigated by computational methods and complex **A** was found to be the lowest energy isomer (SI, Table S8) among the six possible geometrical isomers.[46] Based on the computational investigations, it is proposed that the *in situ* generated active species **A** forms a π-bond with the olefin to yield species **B** (Scheme 1), which inserts into the Fe-H bond to give the metal-alkyl complex **C**. The next step is the formation of the acyl intermediate **D**. Upon addition of H_2, **D** releases the aldehyde and regenerates the active species **A**. In our attempts to trap the acyl intermediate, a reaction between **1** and 1-hexene was conducted at 0 °C to obtain the acyl intermediate **D**. The acyl complex **D** was then treated with iodine in methanol to obtain methyl heptanoate, which was characterized by NMR (SI, Fig. S37), ESI-MS (SI, Fig. S38) and GC-MS (SI, Fig. S39). The observation of methyl heptanoate confirms the intermediacy of species **D**. Similar evidence was presented for the cobalt catalyzed hydroformylation mechanism by Heck and Breslow.[47] Thus, formation and intermediacy of **A** has been demonstrated by various experimental methods and it is therefore reasonable to believe that complex **A** is the actual active species. The observation of the methyl heptanoate further supports the proposed mechanism.

A radical mechanism with a potential radical species $[\bullet Fe(CO)_4^-]$ has also been evoked in the past.[9,48] However, the existence of the radical mechanism seems unlikely based on three experimental pieces of evidence. (a) Two control experiments were performed in the presence of excess (150 times) radical scavengers 2,2,6,6-Teramethylpiperidinyloxy (TEMPO) and galvinoxyl (SI, section 6). In both these cases, the aldehyde product was obtained. If a radical mechanism had been operating, the radical would have been scavenged by TEMPO or galvinoxyl and there would not have been any aldehyde formation. Thus, the formation of aldehyde in the presence of the radical scavenger rules out the possibility of a radical mechanism. (b) *In situ* NMR investigations could be performed without any paramagnetic NMR resonances. The absence of a paramagnetic species further supports the absence of a radical mechanism. (c) CV experiments indicated two electron processes and, therefore, intermediacy of one electron transformations is unlikely.

To obtain detailed insight into the iron catalyzed hydroformylation reaction, full quantum chemical calculations have been performed with density functional theory (DFT) at the PBE/TZVP level of theory. It is well known that an octahedral complex with a general formula MA2B2C2 has six different stereoisomers,[49] and from the calculations, it is found that **A** is the most favorable stereoisomer for $[Fe(CO)_2(H)_2(PPh_3)_2]$ (Fig. 3). The insertion of olefin from the π-complex intermediate **B** can follow two pathways: 1,2-insertion (Path **A**) or 2,1-insertion (Path **B**) (Fig. 3). The former would lead to the linear aldehyde **7a**, while the latter would produce the branched aldehyde **7b**. The energy barriers for this particular step (insertion or hydride transfer) suggested that the 1,2-insertion is more favorable (by 1.3 kcal/mol) (Fig. 4, bottom) for 1-hexene. However, an opposite trend is seen in the case of styrene, where the 2,1-insertion is favored (by 1.7 kcal/mol) (Fig. 4, bottom). These computational findings complement

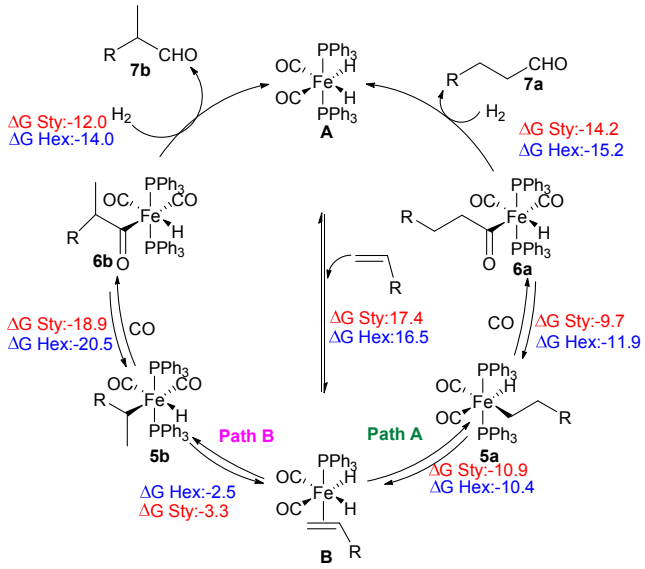

Figure 3. The reaction mechanism for the hydroformylation of olefins calculated at the PBE/TZVP level of theory. ΔG (in kcal/mol) represents Gibbs free energy of reaction.

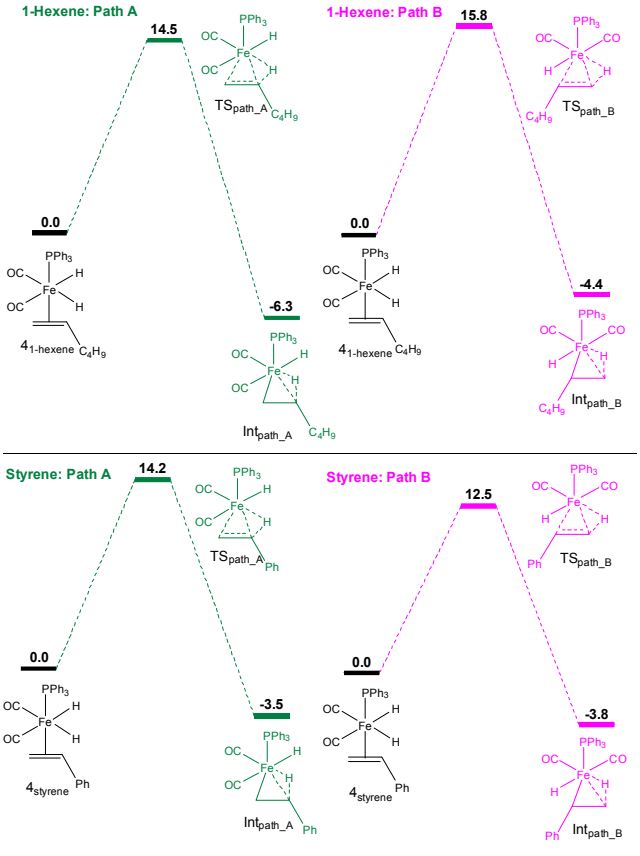

Figure 4. Free energy profile for the hydride transfer step in path **A** and path **B**. The free energy values are in kcal/mol.

the experimental observations, wherein higher amount of branched product was observed for styrene (Table 2, run 12) and the linear product was seen to be the major one for 1-hexene (Table S3, run 1).

Is it Iron or Rhodium?

Iron catalyzed cross-coupling reactions such as "arylation" were reported to be influenced by presence of copper impurities in the Iron precursor $FeCl_3$.[50] In this context; we pondered about the possible role of rhodium impurities in our iron precursor.[51] Thus, a three prong approach was used to establish if it is Iron or Rhodium that is catalyzing the hydroformylation reaction. i) In the first approach, commercially available iron precursor [$Fe_2(CO)_9$] was evaluated in the hydroformylation of 1-octene, in presence and absence of phosphine ligand under identical conditions and the results are presented in table 4. As evident, no hydroformylation was observed with [$Fe_2(CO)_9$] and a meager 1% hydroformylation product (Fig. S46) was observed in presence of triphenyl phosphine ligand. Had there been any rhodium impurity in the commercial precursor [$Fe_2(CO)_9$], it would have catalyzed the HF in presence of triphenyl phosphine ligand. Thus, the lack of hydroformylation in the above experiment suggests that the impurities in the commercial precursor do not catalyze hydroformylation. ii) In the catalyst preparation step, [$Fe_2(CO)_9$] was converted into [$Fe(CO)_5$], which is subsequently utilized for the synthesis of complex **1**. In order to further investigate the role of rhodium impurity in this intermediate, [$Fe(CO)_5$] catalyzed hydroformylation of 1-octene with and without triphenyl phosphine under identical conditions was examined. In this case as well, almost no hydroformylation was observed (Fig. S47). These observations rule out the possible hydroformylation by rhodium impurities and support the assumption that the reaction is most likely catalyzed by Iron. iii) In our attempts to detect the rhodium, the iron precursor [$Fe_2(CO)_9$] and complex **1** were subjected to bulk analyses using atomic absorption/emission spectroscopy and surface analysis using XPS. Both of these analyses revealed absence of rhodium in the precursor (see supporting information section 8). Thus, it is most likely that the hydroformylation is catalyzed by iron and it is highly unlikely that the rhodium impurity that is beyond the detection limits (0.01 ppm) is responsible for the observed HF.

Table 4. Hydroformylation of 1-octene with iron in presence and absence of ligand.[a]

Run	Fe-precursor	Ligand	L:M	Conv. (%)[b]
1	[$Fe_2(CO)_9$]	NA	2.5	0
2	[$Fe_2(CO)_9$]	PPh_3	2.5	~1
3	[$Fe(CO)_5$]	NA	2.5	0
4	[$Fe(CO)_5$]	PPh_3	2.5	0

[a]Conditions: [$Fe_2(CO)_9$]: 0.0109 mmol, [$Fe(CO)_5$]: 0.0204 mmol, Sub/Fe: 100, Solvent: 1 ml methanol, CO/H_2: 20 bars, Temp.: 100 °C, Time : 24 hours; NA: Not added; [b]Determined by GC.

CONCLUSIONS

In summary, the current work unveils a new iron catalyst for the hydroformylation of aliphatic and aromatic olefins under mild conditions. An iron hydride precursor **1**, in combination with readily available phosphine or phosphite ligand and syngas, generates the catalytically active species (which is believed to be **A**) and delivers hydroformylation of 1-hexene, 1-octene, 1-decene, 1-dodecene, 1-octadecene, trimethoxy(vinyl)silane, trimethyl(vinyl)silane, cardanol, 2,3-dihydrofuran, allyl malonic acid, styrene, 4-methyl styrene, 4-*i*Bu-styrene, 4-*t*Bu-styrene, 4-methoxy styrene, 4-acetoxy styrene, 4-bromo styrene, 4-chloro styrene, 4-vinylbenzonitrile, 4-vinylbenzoic acid, and allyl benzene. The reaction operates under relatively mild conditions of 100 °C and 10-30 bars syngas pressure within 24-48 hours. Initial optimization studies with 1-octene indicated an optimal ligand to metal ratio of 2.5, methanol as the most suitable solvent, and a temperature of 100 °C. Short chain 1-hexene could be hydroformylated at 10 bars syngas pressure and 80 °C. While long-chain olefins S3-S5 (C10-C18) required slightly higher syngas pressure of 30 bars to achieve excellent conversion to corresponding aldehydes. The scope of iron catalyzed hydroformylation was extended to functional olefins, cyclic olefins, vinyl aromatics and the hydroformylation S1-S21 was examined. Compared to the aliphatic olefins, vinyl aromatics required longer reaction times. The catalyst tolerated electron donating as well as electron withdrawing functional groups and displayed good to excellent yields. Notable branched selectivity was observed for styrenic substrates (S11-S20), along with significant yields. The addition of 1 mol% of acetic acid was found to promote the hydroformylation reaction and the reaction time for vinyl aromatics could be reduced to 24 hours.

Combined experimental and computational investigations indicate that the di-hydride species **A** is the actual active catalytic species. The identity of species **A** was established by multiple NMR experiments, which indicated coordination of ligand **L1** and formation of the iron-dihydride complex. Cyclic voltammetry results revealed a Fe(0) to Fe(II) interconversion, explaining the accelerating effect of acetic acid. Control experiments with externally added radical scavengers ruled out the possibility of a radical or an Fe(I) to Fe(III) mechanism. The experimental findings were further corroborated by DFT calculations. Among the six possible stereoisomers of iron-dihydride complex, species **A** was found to be the most favorable. Transition state calculations for 1-hexene insertion revealed that 1,2-insertion was favored by 1.3 kcal/mol, whereas styrene preferred 2,1-insertion by 1.7 kcal/mol. Thus, experimental and computational investigations establish that the iron catalyzed hydroformylation follows a Fe(II) catalytic cycle, as depicted in Scheme 1. The role of rhodium impurities in catalyzing the hydroformylation of alkenes was investigated. These studies established that the reported hydroformylation is catalyzed by iron and it is highly unlikely that the rhodium impurities are responsible for the observed hydroformylation.

EXPERIMENTAL SECTION

Materials and methods. Unless noted otherwise, all manipulations were carried out under an inert atmosphere of argon using standard Schlenk line techniques or M-Braun glove box. Tetrahydrofuran was distilled from sodium/benzophenone under argon atmosphere. Methylene chloride was distilled on calcium-hydride. Methanol, ethanol, and isopropanol were dried on magnesium cake. Magnesium turning, triphenyl phosphine, triphenyl phosphite were purchased from Sigma-Aldrich and used without further purification. 1-hexene, 1-octene, 1-decene, 1-dodecene, 1-octadecene, sty-

rene, 4-chloro styrene, trimethoxy(vinyl)silane, trimethyl(vinyl)silane, allyl malonic acid, 4-*t*Bu-styrene, 4-acetoxy styrene, 4-vinylbenzonitrile, 4-vinylbenzoic acid and allyl benzene were purchased from Sigma-Aldrich and used after passing through a plug of neutral alumina followed by distillation. Cashew nut shell liquid was received from Sunshield Chemicals Limited (subsidiary of Solvay) and was further purified to obtain cardanol. 4-*iso*-butyl-styrene was prepared by following a known procedure.[52] $[Fe_2(CO)_9]$, 4-methoxy styrene, 4-methyl styrene, 4-bromo styrene were obtained from Alfa Aesar. Complex $[HFe(CO)_4][PPN]$ (**1)** was synthesized by modifying literature procedure.[13] $[(PPh_3)_2Fe(CO)_3]$ (**iii**) was prepared by following a reported procedure.[42] Other chemicals like methylene chloride, methanol, ethanol, isopropanol, 1,4-dioxane, tetrahydrofuran, toluene, chloroform, calcium hydride, 2,3-dihydrofuran, etc. were purchased from local suppliers. Acetic acid (glacial) was purchased from Qualigens Fine Chemicals and was dried by adding acetic anhydride (7:3). The syngas and hydrogen gas were supplied by Ms. Vadilal Chemicals Ltd, Pune, India. The hydroformylation of α-olefins was run in an Amar Equipment Pvt. Ltd. high pressure reactor equipped with pressure regulators and safety rupture valve. The hydroformylation of 1-octene with incubation was run in an Amar Equipment Pvt. Ltd. high pressure reactor equipped with additional high pressure liquid charging chamber, pressure regulators and safety rupture valve. NMR spectra were recorded on Bruker 200, 400, and 500 MHz instruments. Chemical shifts are referenced to external reference TMS (^{1}H and ^{13}C) or 85% H_3PO_4 (Ξ = 40.480747 MHz, ^{31}P). Coupling constants are given as absolute values. Multiplicities are given as follows s: singlet, d: doublet, t: triplet, m: multiplet. *In-situ* high pressure NMR was recorded in Wilmad quick pressure valve NMR tube. Mass spectra were recorded on Thermo scientific Q-Exactive mass spectrometer; with Hypersil gold C18 column (150 x 4.6 mm diameter 8 μm particle size mobile phase used is 90% methanol + 10 % water + 0.1 % formic acid). IR spectrum was recorded on Bruker alpha-T spectrometer in liquid state. Sample was dissolved in chloroform and spectrum was obtained using sodium chloride window. GC analyses for 1-hexene, 1-octene, 1-decene, 1-dodecene, 1-octadecene, styrene, 4-methoxy styrene, 4-bromo styrene, 4-methyl styrene, other styrenic substrates and allyl benzene were carried out on an Agilent 7890B GC system. GC-MS analysis was carried out on a Varian 3800 GC-MS (Saturn 2000MS) with VF-5 capillary column (5% phenyl, 95% dimethyl polysiloxane). The column oven program used is same as that for GC analysis. Headspace GC analysis was performed on an Agilent 7890A GC system equipped with Porapak column and thermal conductivity detector. Inlet temperature was maintained at 150 °C, column flow = 14 ml/min. Detector temperature was maintained at 200 °C. Temperature program: starting at 60 °C with hold time of 5 mins. Ramp 1: @ 10 °C to 100 °C, hold for 21 mins. Retention time for H_2 = 1.5 mins. The XPS measurements were carried out using Thermo Scientific Kalpha+ spectrometer using a monochromatic Al Kα (1486.6 eV) x-ray source. The base pressure of the spectrometer was 2×10^{-9} mbar. The wide area and narrow region scans were acquired using 100 eV and 50 eV pass energy respectively. The bulk analyses for the detection of rhodium impurity was carried out at three different places using; Varian atomic absorption spectrometer, model-220fs (NCL), SPECTRO Analytical Instruments GmbH, Germany, model-ARCOS, Simultaneous ICP Spectrometer (IIT Bombay), and Agilent model-4100 MP-AES.

Synthesis of $[HFe(CO)_4]^-[PNP]^+$ (1). The desired iron precursor $[HFe(CO)_4]^-[PNP]^+$ was prepared by following a literature reported procedure.[13]

^{1}H NMR (500 MHz in $CDCl_3$): δ = -8.52 (s, 1H, Fe-H). **^{13}C NMR** (125 MHz in $CDCl_3$): δ = 161.5 (C=O), 135.0, 133.6, 130.8, 129.2, 128.3. **^{31}P NMR** (500 MHz in $CDCl_3$): δ = 21.02. **IR** (cm^{-1}) = 1870 (C=O). **ESI-MS** (-ve mode): m/z = 168.91 [M] .

General procedure for hydroformylation.[53] In a typical hydroformylation experiment, a stainless steel autoclave (450 mL) equipped with 50 ml high pressure liquid charging chamber, pressure regulator and a safety valve was used. Individual vials were charged with metal precursor $[HFe(CO)_4]^-[PNP]^+$ (5.5 mg, 0.0077 mmol)}, ligand (as in Tables 1-3), solvent (1 ml), substrate (100 equiv.) and stirring bars in a glove box. The vials were transferred to autoclave and the autoclave was purged three times with syngas (CO: H_2 = 1:1) before pressurizing it to the desired pressure. Suitable temperature and pressure was maintained during the reaction. After completion of the reaction, the autoclave was cooled to 0 °C, and excess gas was vented off in a well-ventilated fume-hood. The conversion and regio-selectivity were determined by using gas chromatography (GC) and proton NMR.

1-hexene. GC analysis for 1-hexene was carried out on an Agilent 7890B GC system using HP-05 column (30 m × 320 μm × 0.25 μm), split ratio 30:1, column pressure 10 psi, injector temperature of 260 °C, detector temperature of 330 °C, argon carrier gas. Temperature program: Initial temperature 50 °C, hold for 1 min.; ramp 1: 4 °C/min. to 120 °C; ramp 2: 20 °C/min. to 250 °C; ramp 3: 20 °C/min. to 320 °C, hold for 2 min. Retention time for 1-hexene = 2.05 min hydrogenated product (n-hexane) = 2.07 min.; branched aldehydes = 4.74 min.; linear aldehyde = 5.65 minute (SI Fig. S7).

1-octene. Temperature program: Initial temperature 70 °C, hold for 1 min.; ramp 1: 4 °C/min. to 120 °C; ramp 2: 10 °C/min. to 250 °C; ramp 3: 20 °C/min. to 320 °C, hold for 2 min. Retention time for 1-octene = 2.7 min.; hydrogenated product (n-octane) = 2.8 min.; branched aldehydes = 7.02 min.; linear aldehyde = 8.1 minute (SI Fig. S6).

1-decene, 1-dodecene, 1-octadecene. Temperature program: Initial temperature 70 °C, hold for 1 min.; ramp 1: 4 °C/min. to 120 °C; ramp 2: 10 °C/min. to 250 °C; ramp 3: 20 °C/min. to 320 °C, hold for 2 min. Retention time for 1-decene = 5.4 min. hydrogenated product (n-decane) = 5.7 min.; branched aldehydes = 13.1 min.; linear aldehyde = 14.4 minute (SI Fig. S8). Retention time for 1-dodecene = 9.9 min. hydrogenated product (n-dodecane) = 11.2 min.; branched aldehydes = 18.0 min.; linear aldehyde = 18.8 min. (SI Fig. S9). Retention time for 1-octadecene = 22.4 min.; branched aldehydes = 26.0 min.; linear aldehyde = 26.5 min. (SI Fig. S10).

Styrene, 4-methyl styrene. GC analysis for styrene and 4-methyl styrene was carried out on an Agilent 7890B GC system using Supelco β-dex 225 (30 m* 0.25 mm * 0.25 μm), split ratio 30:1, column pressure 10 psi., injector temperature of 220 °C, detector temperature of 300 °C, argon carrier gas. Temperature program: Initial temperature 100 °C, hold for 2 min.; ramp 1: 2 °C/min. to 160 °C; ramp 2: 20 °C/min. to 210 °C; hold for 2 min. Retention time R_t for styrene = 7.3 mins.

for hydrogenated product (Ethyl benzene) = 6.3 mins, n-dodecane = 14.7 min. (internal standard), for branched aldehydes = 17.0 mins. for linear aldehyde = 23.2 mins. (SI Fig. S16). Retention time R_t for 4-methyl styrene = 10.3 mins. for branched aldehydes = 22.0 mins. for linear aldehyde = 22.7 mins. (SI Fig. S17).

4-methoxy styrene, 4-bromo styrene, 4-*i*Bu-styrene, 4-*t*Bu-styrene, 4-acetoxy styrene, 4-bromo styrene, 4-chloro styrene, 4-vinylbenzonitrile and allyl benzene. GC analyses for above styrenic substrates was carried out on an Agilent 7890B GC system using Supelco β-dex 225 (30 m* 0.25 mm * 0.25 μm), split ratio 30:1, column pressure 10 psi., injector temperature of 220 °C, detector temperature of 300 °C, argon carrier gas. Temperature program: Initial temperature 100 °C, hold for 2 min.; ramp 1: 2 °C/min. to 160 °C; ramp 2: 10 °C/min. to 210 °C; hold for 2 min. Retention time R_t for 4-methoxy styrene = 20.5 mins. for branched aldehydes = 33.3 mins. for linear aldehyde = 36.0 mins. (SI Fig. S20). Retention time R_t for 4-bromo styrene = 19.3 mins. for branched aldehydes = 35.4 mins. for linear aldehyde = 38.5 mins. (SI Fig. S22). Retention time R_t for 4-*iso*-butyl styrene = 20.7 mins. for branched aldehydes = 32.6 mins. for linear aldehyde = 37.1 mins. (SI Fig. S18). Retention time R_t for 4-tertbutyl styrene = 19.9 mins. for branched aldehydes = 33.3 mins. for linear aldehyde = 36.2 mins. (SI Fig. S19). Retention time R_t for 4-acetoxy styrene = 30.0 mins. for branched aldehydes = 32.9 mins. for linear aldehyde = 38.44 mins. (SI Fig. S21). Retention time R_t for 4-chloro styrene = 14.4 mins. for branched aldehydes = 31.4 mins. for linear aldehyde = 36.0 mins. (SI Fig. S23). Retention time R_t for 4-vinylbenzonitrile = 28.3 mins. for branched aldehydes = 37.0 mins. for linear aldehyde = 38.5 mins. (SI Fig. S24). Retention time R_t for allyl benzene = 8.4 mins. for branched aldehydes = 24.3 mins. for linear aldehyde = 29.2 mins. (SI Fig. S25).

Mechanistic investigations. Coordination of L1 followed by generation of iron-dihydride complex A. In a dried and argon cooled Schlenk tube 0.010 g (0.0000138 moles) of **1** was dissolved in 0.4 ml $CDCl_3$ and 2 equivalent (0.0073 g, 0.0000277 moles) triphenyl phosphine (**L1**) was added to above mixture and the resultant solution was transferred to a high pressure NMR tube. The above mixture was heated to 50 °C for 45 minutes and 45 °C for 16 hours, and the NMR was recorded at 45 °C (SI Fig. S27).

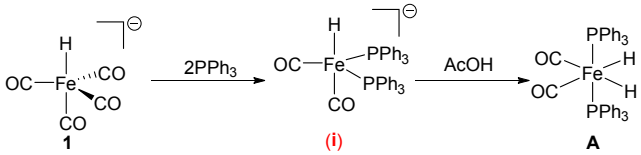

Key resonances of (**i**).

^{31}P NMR (500 MHz, $CDCl_3$): δ = 82.4 (s), 71.6 (s).

Having observed **L1** coordination, the NMR tube was allowed to freeze to liquid nitrogen temperature. Now acetic acid (50 μL) was added to above NMR tube under frozen condition and a proton NMR was recorded at 0 °C immediately. A very weak hydride resonance appeared at -12.2 ppm. The new hydride signal may be attributed to a di-hydride species **A**. Room temperature treatment of **1** with **L1** and acetic acid revealed a doublet at -9.50 ppm (SI, Fig. S33).

Key resonances of **A**.

At 45 °C: **^{31}P NMR** (500 MHz, $CDCl_3$): δ = 81.07 (s). **^{1}H NMR** (500 MHz, $CDCl_3$): δ = -12.28. At room temperature (25 °C): **^{31}P NMR** (500 MHz, $CDCl_3$): δ = 71.5 (s). **^{1}H NMR** (500 MHz, $CDCl_3$): δ = -9.50 (d, $^{2}J_{P\text{-}H}$ = 43 Hz).

Formation of iron-dihydride complex (ii). The iron precursor $[HFe(CO)_4][PPN]$ (**1**) (0.016 g, 0.000022 moles) was dissolved in 0.6 ml $CDCl_3$:MeOH (3:1) mixture in an NMR tube and the tube was cooled to liquid nitrogen temperature. Excess (50 μL) (0.00087 moles) amount of acetic acid was added to above solution at -196 °C. An immediate colour change from light brown to dark red was observed, indicating the change in oxidation state of the metal. The NMR tube was taken out from the liquid nitrogen bath just before inserting it in the magnet and recording the NMR spectrum.

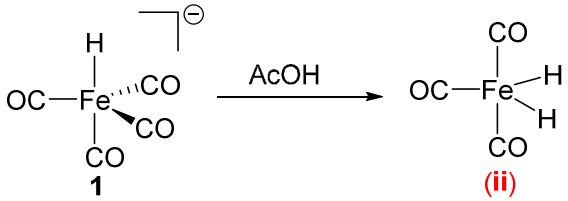

Key resonances of (**ii**).

^{1}H NMR (500 MHz, $CDCl_3$): δ = -15.38.

$[Fe(CO)_3(PPh_3)_2]$ to iron dihydride complex (A). 0.010 g (0.0000150 moles) of $[Fe(CO)_3(PPh_3)_2]$ was taken in a high pressure NMR tube and toluene-d_8 (0.3 ml) was added to it. The above NMR tube was pressurized with hydrogen gas (10 bars) and an NMR was recorded.

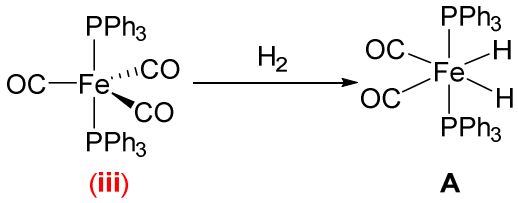

^{31}P NMR (500 MHz, Toluene-d_8): δ = 83.1 (s). **^{1}H NMR** (500 MHz, Toluene-d_8): δ = -8.91 (m), -9.02 (m).

ASSOCIATED CONTENT

Supporting Information. Synthetic procedures, detailed screening tables, characterization data, computational details, NMR spectra, GC chromatograms, control experiments, cyclic voltammetry. This material is available free of charge via the Internet at http://pubs.acs.org.

AUTHOR INFORMATION

Corresponding Author

* Email: s.chikkali@ncl.res.in

ACKNOWLEDGMENT

We gratefully acknowledge the financial support from DST-SERB (SR/S2/RJN-11/2012 and EMR/2016/005120) India, AvH foundation, Bonn and CSIR-NCL, India. SP would like to thank UGC for the senior research fellowship. We thank SAIF-IIT Bomaby, Venture Center, Pune and Dr. Tejas Gaydhankar, NCL Pune for Atomic Absorption/Emission Spectroscopy analysis.

REFERENCES

(1) For recent reviews on hydroformylation see: (a) Torres, G. M.; Frauenlob, R.; Franke, R.; Boerner, A. *Catal. Sci. Technol.* **2015**, *5*, 34-54. (b) Deng, Y.; Wang, H.; Sun, Y.; Wang, X. *ACS Catal.* **2015**, *5*, 6828-6837. (c) Chikkali, S. H.; van

der Vlugt, J. I.; Reek, J. N. H. *Coord. Chem. Rev.* **2014**, *262*, 1-15. (d) Vilches-Herrera, M.; Domke, L.; Boerner, A. *ACS Catal.* **2014**, *4*, 1706-1724. (e) Franke, R.; Selent, D.; Boerner, A. *Chem. Rev.* **2012**, *112*, 5675-5732 and the references therein. (f) van Leeuwen, P. W. N. M.; Kamer, P. C. J.; Claver, C.; Pàmies, O.; Diéguez, M. *Chem. Rev.* **2011**, *111*, 2077-2118.

(2) Kaemper, A.; Kucmierczyk, P.; Seidensticker, T.; Vorholt, A. J.; Franke, R.; Behr, A. *Catal. Sci. Technol.* **2016**, *6*, 8072-8079.

(3) For books, see: van Leeuwen, P. W. N. M. *Homogeneous Catalysis: Understanding the Art*; Kluwer Academic Publishers: Dordrecht, The Netherlands, 2004, pp 125−174.

(4) (a) Duembgen, G.; Neubauer, D. *Chem. Ing. Tech.* **1969**, *41*, 974-980. (b) Bohnen, H. W.; Cornils, B. *Advances in Catalysis*, Vol. 47, Academic Press, New York, 2002, pp. 1-64.

(5) Bohnen, H. W.; Cornils, B. *Adv. Catal.* **2002**, *47*, 1-64.

(6) Claver, C.; van Leeuwen P. W. N. M. *Rhodium Catalyzed Hydroformylation*, Springer, Berlin, 2008 and the references therein.

(7) Whiteker, G. T.; Cobley, C. J. *Top. Organomet. Chem*, **2012**, *42*, 35-46.

(8) (a) Pospech, J.; Fleischer, I.; Franke, R.; Buchholz, S.; Beller, M. *Angew. Chem. Int. Ed.* **2013**, *52*, 2852-2872. (b) Evans, D.; Osborn, J. A.; Wilkinson, G. *J. Chem. Soc. A* **1968**, 3133-3142.

(9) Note that syngas was not used in this reaction, only CO was used, and H_2 was produced in-situ. For details, see: Reppe, V. W.; Vetter, H. *Justus Liebigs Ann. Chem.***1953**, *582*, 133-161.

(10) Palágyi, J.; Markó, L. *J. Organomet. Chem.* **1982**, *236*, 343-347.

(11) (a) He, Z.; Lugan, N.; Neibecker, D.; Mathieu, R.; Bonnet, J.-J. *J. Organomet. Chem.* **1992**, *426*, 247-259. (b) Along the same lines, a Rh-Fe bimetallic complex was claimed to be responsible for the hydroformylation of 1-hexene, see: Trzeciak, A. M.; Mieczynska, E.; Ziolkowski, J. J. *Topics Catal.* **2000**, *11/12*, 461-468.

(12) Breschi, C.; Piparo, L.; Pertici, P.; Maria Caporusso, A.; Vitulli, G. *J. Organomet. Chem.* **2000**, *607*, 57-63.

(13) (a) Bianchini, C.; Lee, H. M.; Meli, A.; Vizza, F. *Organometallics* **2000**, *19*, 849-853. (b) van der Slot, S. C.; Kamer, P. C. J.; van Leeuwen, P. W. N. M.; Iggo, J. A.; Heaton, B. T. *Organometallics* **2001**, *20*, 430-441. (c) Hettersheid, D. G. H.; Chikkali, S. H; de Bruin, B.; Reek, J. N. H. *ChemCatChem* **2013**, *5*, 2785-2793.

(14) (a) Smith, M. B.; Bau, R. *J. Am. Chem. Soc.* **1973**, *7*, 2388-2389. (b) Brunet, J. J.; Chauvin, R.; Diallo, O.; Kindela, F.; Leglaye, P.; Neibecker, D. *Coord. Chem. Rev.* **1998**, *178-180*, 331-351.

(15) Fuerstner, A. *ACS Cent. Sci.* **2016**, *2*, 778-789.

(16) For recent reports on monodentate phosphines in hydroformylation, see: (a) Mormul, J.; Mulzer, M.; Rosendhal, T.; Romiger, F.; Limbach, M.; Hofmann, P. *Organometallics* **2015**, *34*, 4102-4108. (b) Alsalahi, W.; Grzybek, R.; Trzeciak, A. M. *Catal. Sci. Technol.* **2017**, *7*, 3097-3103.

(17) (a) For review, see reference 1f. (b) Saidi, O.; Ruan, J.; Vinci, D.; Wu, X.; Xiao, J. *Tetrahedron Lett.* **2008**, *49*, 3516-3519.

(18) Deshmukh, S. S.; Gaikwad, S. R.; Pandey, S.; Mali, P.; Chikkali, S. H. *J. Chem. Sci.* **2017**, *129*, 1143-1152.

(19) van Leeuwen, P. W. N. M.; Kamer, P. C. J.; Reek, J. N. H.; Dierkes, P. *Chem. Rev.* **2000**, *100*, 2741-2769.

(20) Chikkali, S. H.; Bellini, R.; Berthon-Gelloz, G.; van der Vlugt, J. I.; de Bruin, B.; Reek, J. N. H. *Chem. Commun.* **2010**, *46*, 1244-1246.

(21) (a) How, R. C.; Hembre, R.; Ponasik, J. A.; Tolleson, G. S.; Clarke, M. L. *Catal. Sci. Technol.* **2016**, *6*, 118-124. (b) Chikkali, S. H.; Bellini, R.; de Bruin, B.; van der Vlugt, J. I.; Reek, J. N. H. *J. Am. Chem. Soc.* **2012**, *134*, 6607-6616. (c) For a general review on this class of ligands in catalysis, see: Chen, X.-S.; Hou, C.-J.; Hu, X.-P. *Synth. Commun.* **2016**, *46*, 917-941.

(22) (a) Noonan, G. M.; Fuentes, J. A.; Cobley, C. J.; Clarke, M. L. *Angew. Chem. Int. Ed.* **2012**, *51*, 2477-2480. (b) Robert, T.; Abiri, Z.; Wassenaar, J.; Sandee, A. J.; Romanski, S.; Neudörfl, J. −M.; Schmalz, H. −G.; Reek, J. N. H. *Organometallics* **2010**, *29*, 478-483. (c) Arribas, I.; Vargas, S.; Rubio, M.; Suárez, A.; Domene, C.; Alvarez, E.; Pizzano, A. *Organometallics* **2010**, *29*, 5791-5804. (d) Rubio, M.; Suárez, A.; Alvarez, E.; Bianchini, C.; Oberhauser, W.; Peruzzini, M.; Pizzano, A. *Organometallics* **2007**, *26*, 6428-6436. (e) Slagt, V. F.; Röder, M.; Kamer, P. C. J.; van Leeuwen, P. W. N. M.; Reek, J. N. H. *J. Am. Chem. Soc.* **2004**, *126*, 4056-4057. (f) Arena, C. G.; Faraone, F.; Graiff, C.; Tiripicchio, A. *Eur. J. Inorg. Chem.* **2002**, 711-716. (g) Beghetto, V.; Scrivanti, A.; Matteoli, U. *Catal. Commun.* **2001**, *2*, 139-143. (h) Deerenberg, S.; Kamer, P. C. J.; van Leeuwen, P. W. N. M. *Organometallics* **2000**, *19*, 2065-2072. (i) Nozaki, K.; Sakai, N.; Nanno, T.; Higashijima, T.; Mano, S.; Horiuchi, T.; Takaya, H. *J. Am. Chem. Soc.* **1997**, *119*, 4413-4423.

(23) Many of the commercial plants for hydroformylation use these simple ligands.

(24) See supporting information Table S1 for detailed screening and experimental procedure etc.

(25) For a review on the role of phosphites in hydroformylation, see: Diéguez, M.; Pàmies, O.; Claver, C. *Tetrahedron: Asymmetry*, **2004**, *15*, 2113-2122.

(26) (a) Foca, C. M.; Barros, H. J. V.; dos Santos, E. N.; Gusevskaya, E. V.; Bayon, J. C. *New J. Chem.* **2003**, *27*, 533-539. (b) Janecko, H.; Trzeciak, A. M.; Ziolkowski, J. J. *J. Mol. Catal.* **1984**, *26*, 355-361. (c) Pittman-Jr., C. U.; Honnick, W. D. *J. Org. Chem.* **1980**, *45*, 2132-2139.

(27) For hydroformylation of 1-decene, see: (a) Hamerla, T.; Rost, A.; Kasaka, Y.; Schomäcker, R. *ChemCatChem* **2013**, *5*, 1854-1862. (b) Markert, J.; Brunsch, Y.; Munkelt, T.; Kiedorf, G.; Behr, A.; Hamel, C.; Seidel-Morgenstern, A. *Appl. Catal. A: Gen.* **2013**, *462-463*, 287-295.

(28) Hydroformylation of higher alkenes is a challenging task, see: (a) Kunene, T. E.; Webb, P. B.; Cole-Hamilton, D. J. *Green Chem*. **2011**, *13*, 1476-1481. (b) Potier, J.; Menuel, S.; Monflier, E.; Hapoit, F. *ACS Catal.* **2014**, *4*, 2342-2346.

(29) For recent reports on hydroformylation of 1-decene, see: (a) Divekar, S. S.; Deshpande, R. M; Chaudhari, R. V. *Catal. Lett.* **1993**, *21*, 191-200; (b) Takahashi, K.; Yamashita, M.; Ichihara, T.; Nakano, K.; Nozaki, K. *Angew. Chem. Int. Ed*. **2010**, *49*, 4488-4490. (c) Takahashi, K.; Yamashita, M.; Tanaka, Y.; Nozaki, K. *Angew. Chem. Int. Ed*. **2012**, *51*, 4383-4387.

(30) For hydroformylation of 1-dodecene, see: (a) Yuan, M.; Chen, H.; Li, R.; Li, Y.; Li, X. *Catal. Lett.* **2004**, *94*, 15-16. (b) Bhange, B. M.; Divekar, S. S.; Deshpande, R. M.; Chaudhari, R. V. *J. Mol. Catal. A: Chem*. **1997**, *115*, 247-257.

(31) Hydroformylation of 1-octadecene is rarely reported, see: Koch, T. J.; Desset, S. L.; Leitner, W. *Green Chem.* **2010**, *12*, 1719-1721.

(32) For rhodium catalyzed hydroformylation of styrene, see: (a) Nelsen, E. R.; Landis, C. R. *J. Am. Chem. Soc*. **2013**, *135*, 9636-9639. (b) Brezny, A. C.; Landis, C. R. *J. Am. Chem. Soc*. **2013**, *139*, 2778-2785. (c) Tonks, I. A.; Froese, R. D.; Landis, C. R. *ACS Catal.* **2013**, *3*, 2905-2909. (d) Boymans, E.; Janssen, M.; Müeller, C.; Lutz, M.; Vogt, D. *Dalton Trans*. **2013**, *42*, 137-142. (e) Jing, Q.; Kazlauskas, R. J. *ChemCatChem* **2010**, *2*, 953-957.

(33) van Rooy, A.; Orij, E. N.; Kamer, P. C. J.; van Leeuwen, P. W. N. M. *Organometallics* **1995**, *14*, 34-43 and the references therein.

(34) For linear selective hydroformylation of styrene, see: Kranenberg, M.; van der Burgt, Y. E. M.; Kamer, P. C. J.; van Leeuwen, P. W. N. M.; Goubitz, K.; Fraanje, J. *Organometallics* **1995**, *14*, 3081-3089 and the reference therein.

(35) For hydroformylation of 4-methoxy styrene, see: Kadyrov, R.; Heller, D.; Selke, R. *Tetrahedron: Asymmetry* **1998**, *9*, 329-340.

(36) For recent representative example of hydroformylation of 4-methyl styrene, see: Doro, F.; Reek, J. N. H.; van Leeuwen, P. W. N. M. *Organometallics* **2010**, *29*, 4440-4447.
(37) Kollar, L.; Farkas, E.; Batiu, J. *J. Mol. Catal. A: Chem.* **1997**, *115*, 283-288.
(38) Siegel, H.; Himmele, W. *Angew. Chem. Int. Ed.* **1980**, *19*, 178-183.
(39) Additive effect was evaluated with an additive to [Fe] ratio of 1, 2, 5. 1 equivalent acetic acid was found to promote the hydroformylation, while excess acetic acid seems to have deleterious effect, see supporting information.
(40) See reference 9, 10 and Sanchez-Delgado, R. A.; Bradley, J. S.; Wilkinson, G. *J. Chem. Sci. Dalton Trans.* **1976**, 399-404.
(41) Bellagamba, V.; Ercoli, R.; Gamba, A. *J. Organomet. Chem.* **1982**, *235*, 201-214.
(42) Boddien, A.; Loges, B.; Gärtner, F.; Torborg, C.; Fumino, K.; Junge, H.; Ludwig, R.; Beller, M. *J. Am. Chem. Soc.* **2010**, *132*, 8924-8934.
(43) The observed chemical shifts are consistent with those reported for $[H_2Fe(CO)_2(dppe)]$, $[H_2Fe(CO)_2(PPh_3)_2]$, $[H_2Fe(CO)_2\{P(OR)_3\}_2]$, see: (a) Schubert, U.; Knorr, M. *Inorg. Chem.* **1989**, *28*, 1765-1766. (b) Cenini, S.; Porta, F.; Pizzotti, M. *Inorg. Chima. Acta.* **1976**, *20*, 119-126. (c) Porta, F.; Cenini, S.; Giordano, S.; Pizzotti, M. *J. Organomet. Chem.* **1978**, *150*, 261-271. (d) Brunet, J. J.; Kindela, F. B.; Labroue, D.; Neibecker, D**.** *Inorg. Chem.* **1990**, *29,* 4152-4153.
(44) In this step, heating to 50 °C is involved, so as to obtain reasonable phosphine coordination. It is most likely that due to heating, H_2 gas is released leaving no hydride on the metal.
(45) It was observed that addition of acetic acid accelerates the hydroformylation reaction; therefore acetic acid was chosen to investigate the change in oxidation state of iron precursor (**1**).
(46) See supporting information, section 7 for energy optimization, transition state calculations and computational details.
(47) Heck, R.; Breslow, D. *J. Am. Chem. Soc.* **1961**, *83*, 4023-4027.
(48) An organo-catalytic hydroformylation with a radical intermediate has been recently reported, see: Huang, H.; Yu, C.; Zhang, Y.; Zhang, Y.; Mariano, P. S.; Wang, W. *J. Am. Chem. Soc.* **2017**, *139*, 9799-9802.
(49) M. North, in *Principles and applications of stereochemistry*, Stanley Thornes (publishers) Ltd, Cheltenham, UK, 1998.
(50) (a) Buchwald, S. L.; Bolm, C. *Angew. Chem. Int. Ed.* **2009**, *48*, 5586-5587; (b) Plenio, H. *Angew. Chem. Int. Ed.* **2008**, *47*, 6954-6956.
(51) The influence of impurities in a catalytic reaction was pointed out by one of the reviewer and the editor during the reviewing process; we thank both of them for the constructive comments.
(52) Movahhed, S.; Westphal, J.; Dindaroglu, M.; Falk, A.; Schmalz, H.-G. *Chem. Eur. J.* **2016**, *22*, 7381-7384.
(53) A patent has been filed, see: Chikkali, S. H.; Pandey, S. Indian Patent Application: IN2017 11015470.

TOC

Iron Catalyzed Hydroformylation of Alkenes under Mild Conditions: Evidence of an Fe(II) Catalyzed Process

Swechchha Pandey,[a] K. Vipin Raj,[b] Dinesh R. Shinde,[c] Kumar Vanka,[b] Varchaswal Kashyap,[b] Sreekumar Kurungot,[b] Samir H. Chikkali[a,d]*

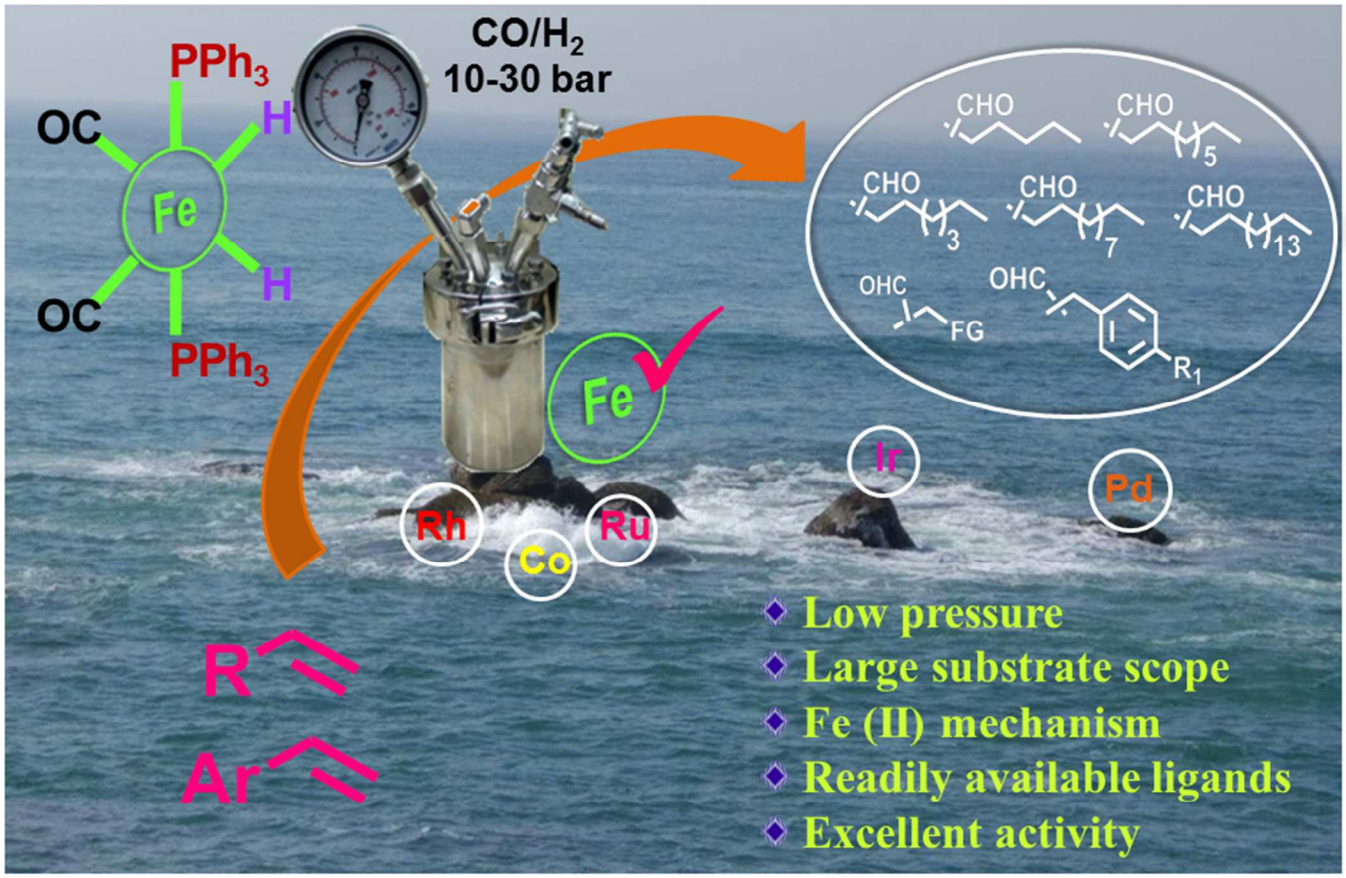

Insert Table of Contents artwork here

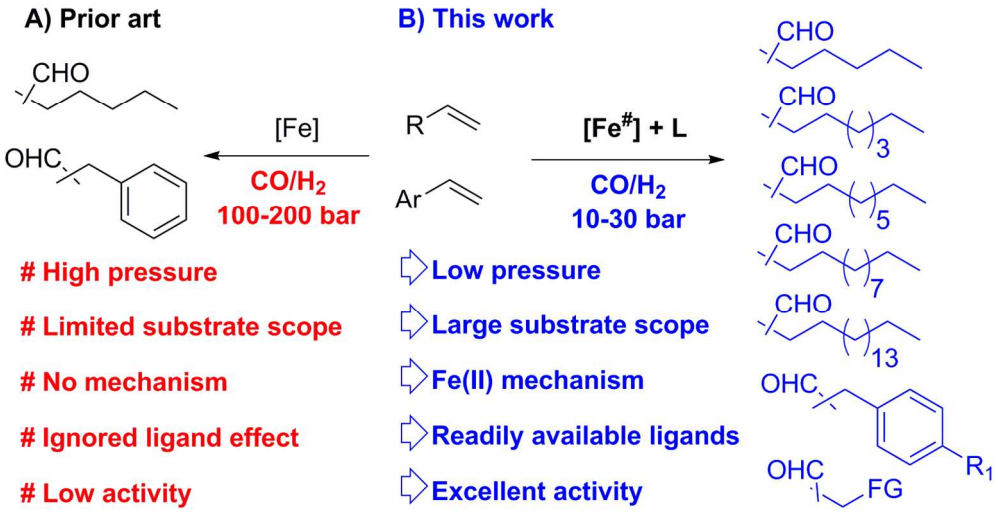

Fig. 1

135x70mm (300 x 300 DPI)

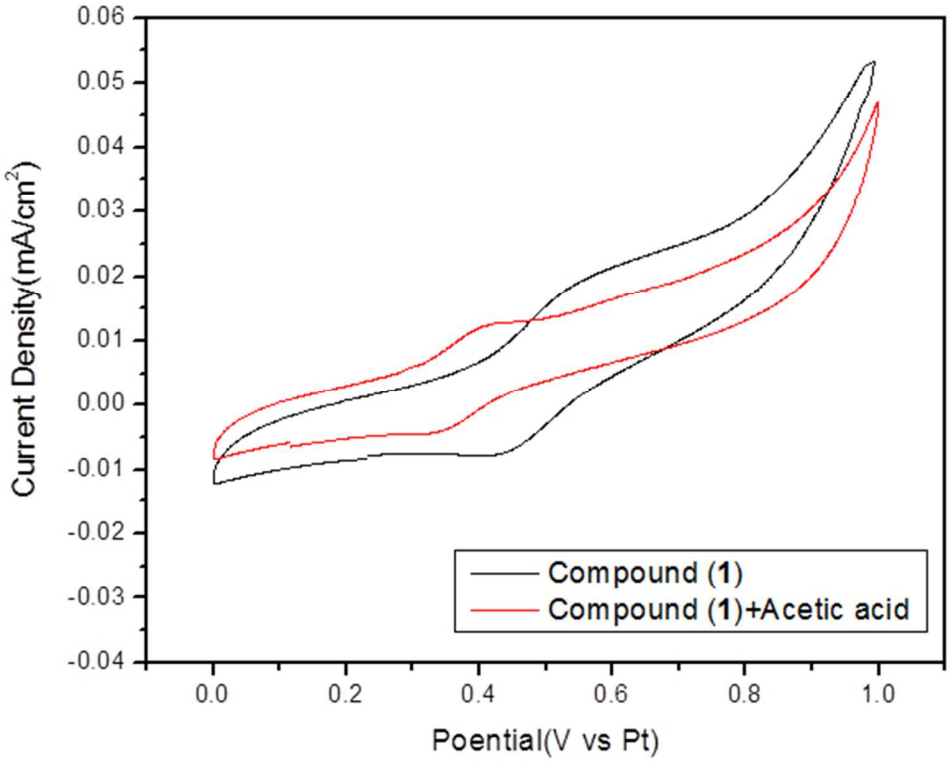

Fig.2

161x125mm (96 x 96 DPI)

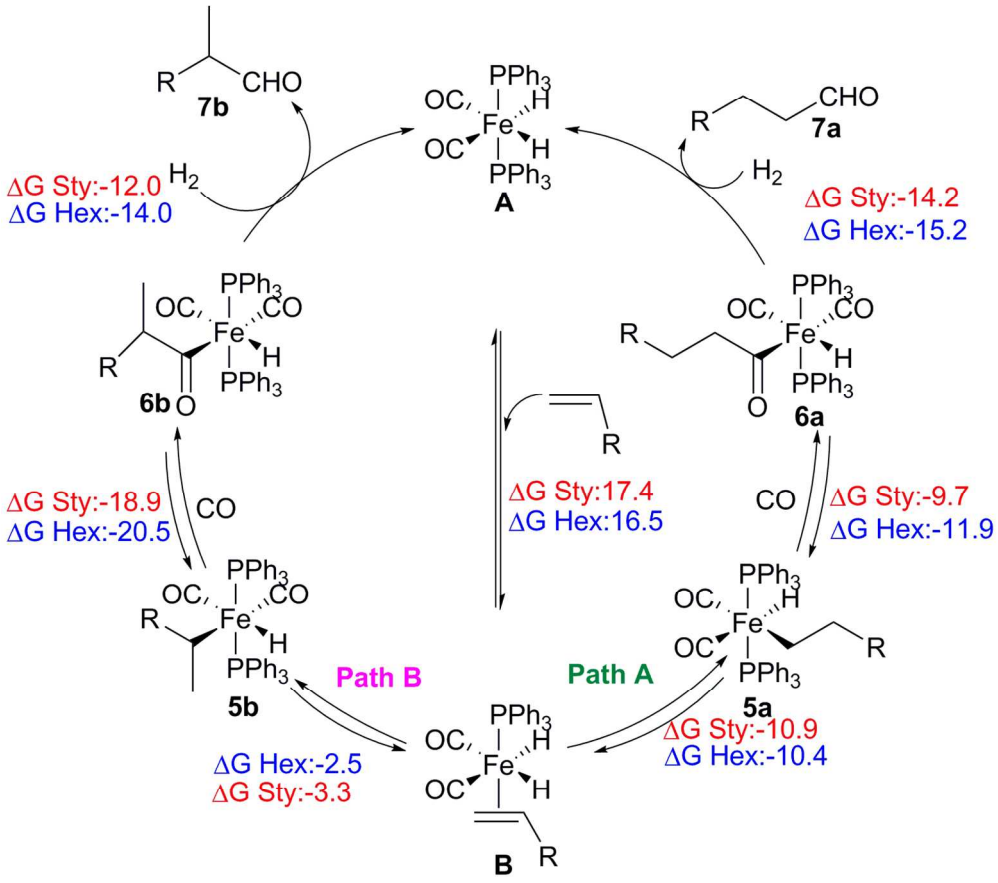

Fig.3

129x114mm (300 x 300 DPI)

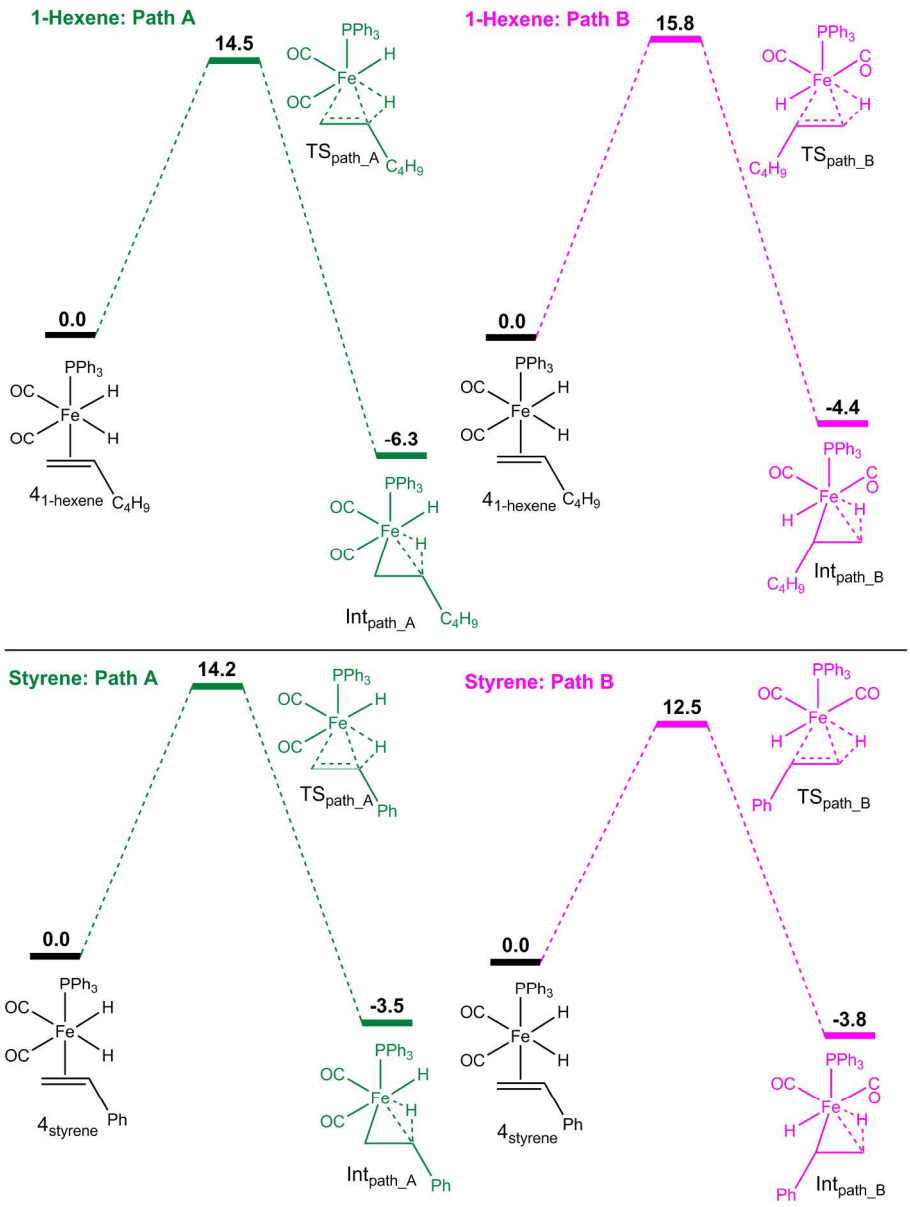

Fig.4

192x252mm (300 x 300 DPI)

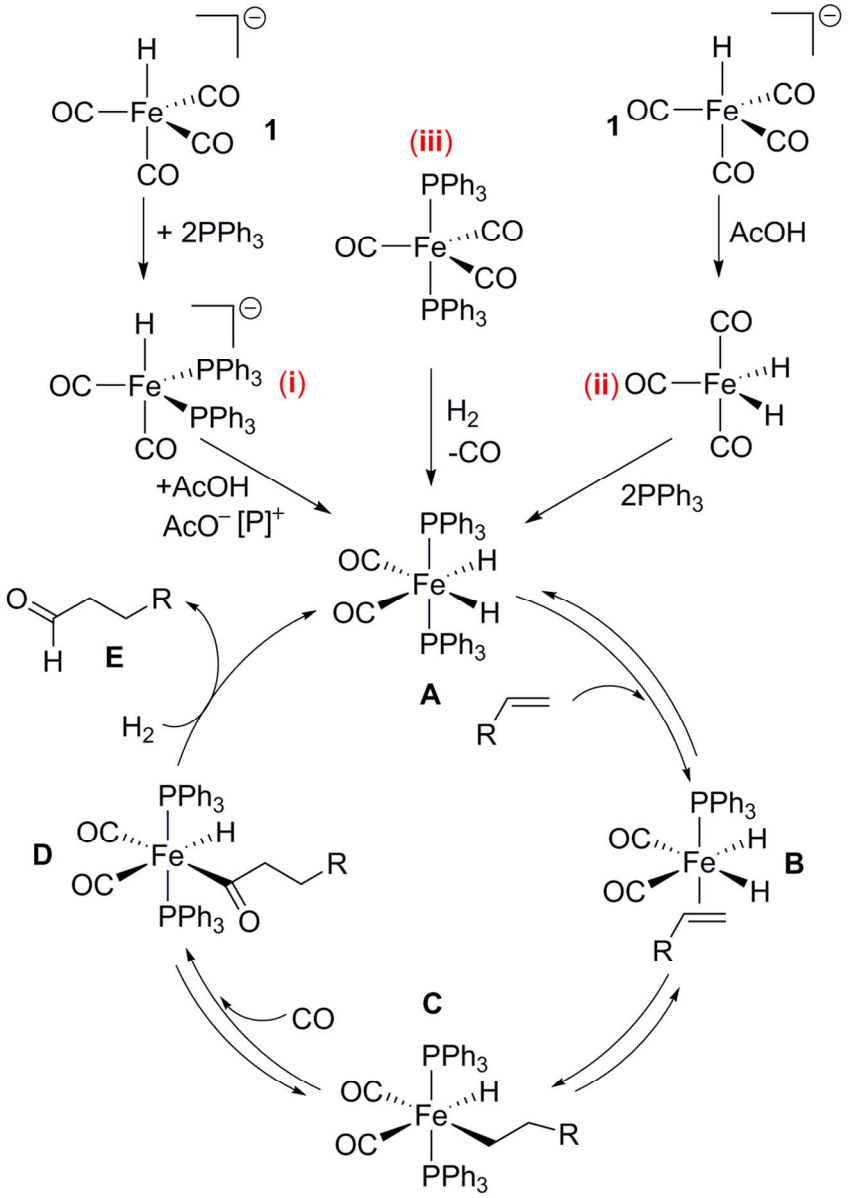

Scheme 1

102x145mm (300 x 300 DPI)

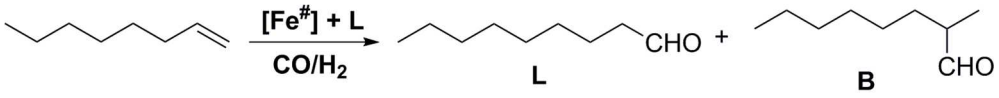

Table 1

137x14mm (300 x 300 DPI)

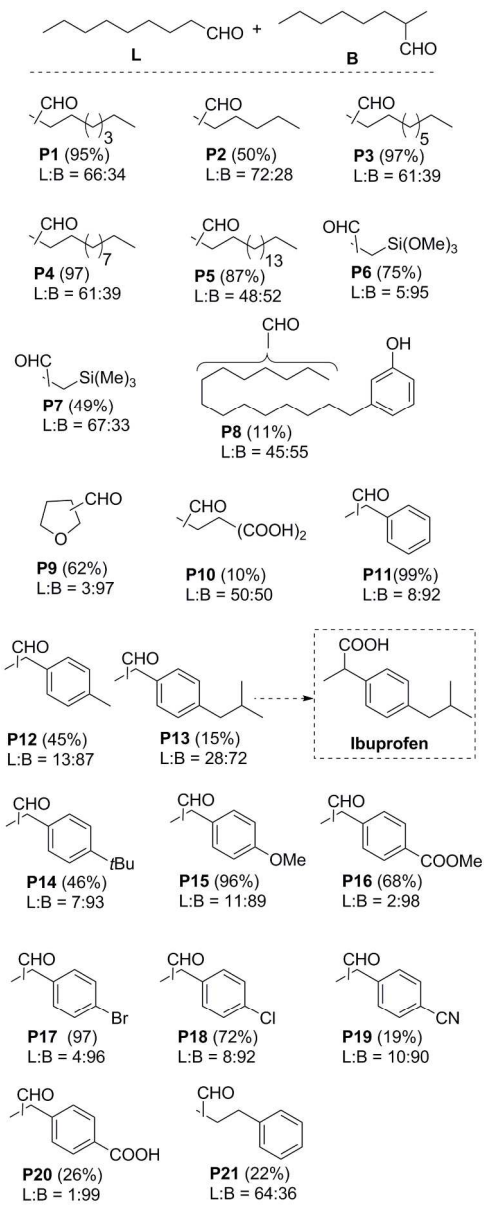

Table 2

100x249mm (300 x 300 DPI)

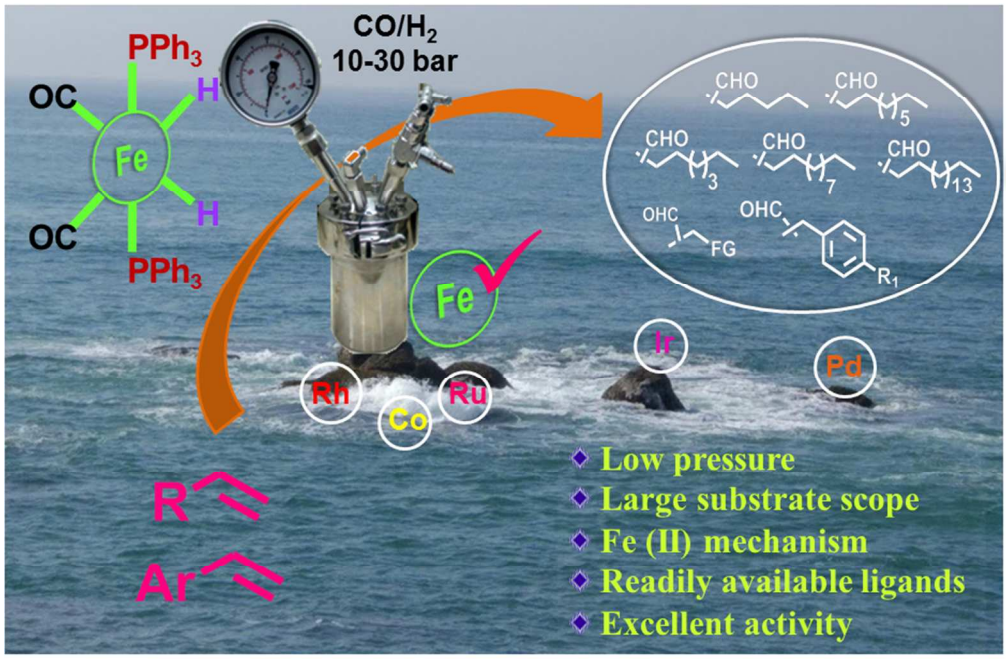

ToC graphic

247x161mm (96 x 96 DPI)